



OPEN

## Structural characterization, biofunctionality, and environmental factors impacting rheological properties of exopolysaccharide produced by probiotic *Lactococcus lactis* C15

Gafar Bamigbade<sup>1</sup>, Abdelmoneim H. Ali<sup>2</sup>, Athira Subhash<sup>1</sup>, Camila Tamiello-Rosa<sup>1</sup>, Farah R. Al Qudsi<sup>3</sup>, Gennaro Esposito<sup>4</sup>, Fathalla Hamed<sup>5</sup>, Shao-Quan Liu<sup>6</sup>, Ren-You Gan<sup>7</sup>, Basim Abu-Jdayil<sup>8</sup>✉ & Mutamed Ayyash<sup>1</sup>✉

Exopolysaccharides (EPSs) possess distinctive rheological and physicochemical properties and innovative functionality. This study aimed to investigate the physicochemical, bioactive, and rheological properties of an EPS secreted by *Lactococcus lactis* subsp. *lactis* C15. EPS-C15 was found to have an average molecular weight of  $8.8 \times 10^5$  Da and was identified as a hetero-EPS composed of arabinose, xylose, mannose, and glucose with a molar ratio of 2.0:2.7:1.0:21.3, respectively. The particle size and zeta potential represented 311.2 nm and  $-12.44$  mV, respectively. FITR exhibited that EPS-C15 possessed a typical polysaccharide structure. NMR displayed that EPS-C15 structure is  $\rightarrow 3)\alpha\text{-d-Glc}^{\text{vi}}(1 \rightarrow 3)\alpha\text{-d-Xyl}^{\text{v}}(1 \rightarrow 6)\alpha\text{-d-Glc}^{\text{iv}}(1 \rightarrow 4)\alpha\text{-d-Glc}(1 \rightarrow 3)\beta\text{-d-Man}(1 \rightarrow 2)\alpha\text{-d-Glc}(1 \rightarrow$ . EPS-C15 scavenged DPPH and ABTS free radicals with 50.3% and 46.4% capacities, respectively. Results show that the antiproliferative activities of EPS-C15 revealed inhibitions of 49.7% and 88.1% against MCF-7 and Caco-2 cells, respectively. EPS-C15 has antibacterial properties that inhibited *Staphylococcus aureus* (29.45%), *Salmonella typhimurium* (29.83%), *Listeria monocytogenes* (30.33%), and *E. coli* O157:H7 (33.57%). The viscosity of EPS-C15 decreased as the shear rate increased. The rheological properties of the EPS-C15 were affected by changes in pH levels and the addition of salts. EPS-C15 is a promising biomaterial that has potential applications in various industries, such as food, pharmaceuticals, and healthcare.

Exopolysaccharides (EPSs) are large, complex, and high-molecular-weight biological macromolecules composed of repeated monosaccharide units. EPSs are classified into two main categories: Hetero-EPS and homo-EPSs depending on their molar ratios and the type of monosaccharide subunits contained. EPSs consisting of identical mono-sugar subunits are referred to as homo-EPSs, while those with varying building blocks are known as hetero-EPSs<sup>1</sup>. The production of EPSs by various microorganisms, such as microalgae, non-filamentous fungi, and bacteria, particularly lactic acid bacteria (LAB), has been extensively studied<sup>2,3</sup>. It was reported that the

<sup>1</sup>Department of Food Science, College of Agriculture and Veterinary Medicine, United Arab Emirates University (UAEU), Al Ain, UAE. <sup>2</sup>Department of Food Science, Faculty of Agriculture, Zagazig University, Zagazig 44511, Egypt. <sup>3</sup>Department of Nutrition and Food Technology, Jordan University of Science and Technology, Irbid 21121, Jordan. <sup>4</sup>Science Division - New York University Abu Dhabi, NYUAD Campus, Saadiyat Island, PO Box 129188, Abu Dhabi, UAE. <sup>5</sup>Department of Physics, College of Science, United Arab Emirates University (UAEU), PO Box 1555, Al Ain, UAE. <sup>6</sup>Department of Food Science and Technology, Faculty of Science, National University of Singapore, Science Drive 2, Singapore 117542, Singapore. <sup>7</sup>Singapore Institute of Food and Biotechnology Innovation (SIFBI), Agency for Science, Technology and Research (A\*STAR), Singapore 138669, Singapore. <sup>8</sup>Chemical and Petroleum Engineering Department, College of Engineering, United Arab Emirates University (UAEU), PO Box 15551, Al Ain, UAE. ✉email: babujdayil@uaeu.ac.ae; mutamed.ayyash@uaeu.ac.ae

characteristics, composition, and structure of EPSs produced by LAB are influenced by the genetic makeup of the bacterial species or strains, as well as the environmental conditions during growth, resulting in different LAB-producing EPSs with distinct pathways and properties<sup>4,5</sup>. For example, *Lactobacillus delbrueckii* subsp. *bulgaricus* and *Streptococcus thermophilus* employ Wzx/Wzy-dependent pathways and extracellular synthetic pathways to produce homo-EPSs and hetero-EPSs, respectively<sup>6</sup>.

EPSs are safe substances, and therefore they are suitable for use in food applications, such as the preservation and enhancement of nutritional and sensory qualities. The growing body of research documenting the various biological activities of microbial EPSs has led to increased interest in their uses across various industries, including foods, pharmaceuticals, cosmetics, and healthcare<sup>7</sup>. These activities have been linked to the physical, chemical, and biological properties of EPSs, which have been shown to exhibit antioxidant, anticancer, and antibacterial properties<sup>8</sup>. Furthermore, the rheological properties of EPSs, such as storage and loss moduli, are considered important parameters during their application in foods and healthcare<sup>9</sup>. Different EPSs have various rheological parameters, and this is determined by the type and substitutions of functional groups, monosaccharide content, molecular weight, and the type of glycosidic bonds<sup>6</sup>. It is a well-established fact that the incidence of non-communicable diseases, such as diabetes and cancer, is increasing globally. The World Health Organization (WHO) predicts that by 2030, the number of global cancer patients will reach 23.6 million, with breast cancer being the most common, although colon cancer will have the highest mortality rate<sup>10,11</sup>. In order to address this public health concern, researchers are actively searching for natural anticancer agents that can mitigate the negative side effects of conventional chemotherapy<sup>12</sup>. Additionally, diabetic patients often experience side effects, such as flatulence and diarrhea, from consuming antidiabetic inhibitors like acarbose, used to control blood sugar levels. Therefore, there is a need for alternative inhibitors of natural origin that do not have known toxic effects<sup>13</sup>.

EPSs produced by LAB offer a variety of antioxidant sources that could be applied in several fields<sup>14</sup>. LAB-EPSs have the possibility of becoming an oral hypoglycemic vehicle to avoid type II diabetes. In addition, EPSs can inhibit  $\alpha$ -amylase and  $\alpha$ -glucosidase activities, decreasing the rate of food hydrolysis to glucose in the intestine, which, by the way, decreases the content of glucose in the blood<sup>15</sup>. LAB-EPSs are also potential antiproliferative substances that have antiproliferative influences on liver, breast, intestinal, and other cancer cells<sup>16</sup>. Simultaneously, LAB-derived EPSs could be applied as a prebiotic to boost human health via a selective improvement of EPS-producing LAB or other probiotic strains and progress the stress tolerance of EPS-forming LAB<sup>14</sup>. Among the different species of LAB, *Lactococcus lactis* subsp. *lactis* is regularly utilized as an industrial starter culture in the manufacture of various dairy products<sup>17</sup>. Significant progress has been achieved in investigating the synthesis of EPS by various lactic acid bacteria, including *Lactococcus lactis*. Specific *eps* gene clusters have been identified and thoroughly characterized in diverse EPS-producing strains of lactococci. EPS produced by *L. lactis* has been reported to improve the texture properties of the cream cheese<sup>18</sup>. Feng et al.<sup>19</sup>, Feng et al.<sup>20</sup> have characterized EPS from two different *Lactococcus lactis* strains (EPS-Q9 and EPS-Z2). This indicates the significance of investigating new EPS produced by novel newly isolated *Lactococcus* spp<sup>21</sup>.

Recently, *L. lactis* C15 (accession number KX881768) was isolated from camel milk, and it was identified as LAB with potential probiotic properties. Different *L. lactis* strains, such as *L. lactis* KX881782 and *L. lactis* KX881768 exhibited remarkable EPS production<sup>22</sup>. However, the characterization of the secreted EPSs was not investigated in detail elsewhere. Therefore, this study aimed to examine the characteristics of EPS-C15, which is produced by the *L. lactis* C15 strain, a potential probiotic. The study investigated the physicochemical properties of EPS-C15, as well as its biological activities, including antioxidant activity, cytotoxicity, and antipathogenic activities. Furthermore, the study evaluated the effects of different salts (CaCl<sub>2</sub> and NaCl) and pH values (4.0 and 6.0) on the rheological properties of EPS-C15.

## Materials and methods

### Materials

*Lactococcus lactis* C15 was isolated from raw camel milk samples on MRS agar and characterized as potential probiotic bacteria by Abushelaibi et al.<sup>22</sup>. It was stored at  $-80\text{ }^{\circ}\text{C}$  in a glycerol solution (50%). M-17 broth (LAB-M Limited, Lancashire, UK) was used to culture *L. lactis* C15, which was sub-cultured several times before the extraction of EPSs. Furthermore, *Staphylococcus aureus* ATCC 15,923, *Salmonella* Typhimurium 02-8423, *Listeria monocytogenes* ATCC 7644, and *Escherichia coli* O157:H7 1934 were obtained from Prof. Richard Holley Laboratory, University of Manitoba, Canada. Trichloroacetic acid (TCA), pullulan standard, xylose, galactose, glucose, arabinose, mannose, 2,2-azino-bis(3-ethylbenzo-thiazoline-6-sulphonic acid (ABTS), 1,1-diphenyl-2-picrylhydrazyl (DPPH),  $\alpha$ -amylase enzyme,  $\alpha$ -glucosidase enzyme, colon carcinoma (Caco-2) cell line, breast carcinoma (MCF-7) cell line, M17 broth, Brain heart infusion (BHI), Deuterium oxide (D<sub>2</sub>O), 0.1 M of CaCl<sub>2</sub>, and 0.1 M of NaCl. All chemicals and microbial media were purchased from Sigma-Aldrich, St. Louis, Missouri, USA.

### EPS-C15 isolation and purification

The extraction of EPS from *L. lactis* C15 was carried out in three stages according to the procedure described by Wang et al.<sup>23</sup>. Firstly, *L. lactis* C15 was grown in M-17 broth media containing 20 g/L of sucrose. Then, the bacterial cells were removed through centrifugation and filtration. The M-17 broth was incubated at  $25.0 \pm 0.1\text{ }^{\circ}\text{C}$  for 48 h and then centrifuged at  $4000 \times g$  for 20 min at  $4\text{ }^{\circ}\text{C}$  to obtain a cell-free supernatant. Chilled absolute ethanol was added to the cell-free supernatant to precipitate the EPS-C15 polymer, which was left at  $4\text{ }^{\circ}\text{C}$  for 24 h. Then, the crude extract was obtained through centrifugation at  $8000 \times g$  for 30 min at  $4\text{ }^{\circ}\text{C}$ . Afterwards, the crude extract was mixed with trichloroacetic acid to reach a final concentration of 8%, for 30 min at room temperature, followed by centrifugation at  $9000 \times g$  for 20 min. Next, the supernatant was dialyzed (MWCO 20 kDa; Slide-A-Lyzer Cassettes, Thermo Fisher Scientific Inc, MA, USA) against dd-water for 48 h at  $4\text{ }^{\circ}\text{C}$ . The partially purified

EPS was freeze-dried at  $-80\text{ }^{\circ}\text{C}$ , and a portion was stored at  $-20\text{ }^{\circ}\text{C}$  in a sealed container for further analysis. A sample was scanned for nucleic acid and protein traces by using a UV-Vis spectrometer (Epoch2, Bio-Tek, VT, USA) at 260 and 280 nm, respectively. No absorbance was detected, indicating the absence of nucleic acids or proteins in the purified EPS-C15.

### EPS-C15 characterization

#### *Average molecular weight and monosaccharides composition*

The average molecular weight of the extracted EPS-C15 was determined by using gel permeation chromatography attached to a refractive index detector (Waters Cooperation, Herts, UK). The molecular weight was estimated by plotting pullulan as an external standard with molecular weights of 5 kDa, 10 kDa, 20 kDa, 50 kDa, and 100 kDa. The detailed procedure was described by Kansandee et al.<sup>24</sup>. The identification of EPS-C15 monosaccharide residues was performed using the traditional acid hydrolysis method. The acid hydrolysis was performed by mixing EPS-C15 with 5 mL of 2.0 M trifluoroacetic acid, followed by heating at  $120\text{ }^{\circ}\text{C}$  for 2 h. The analysis of the monosaccharide composition of EPS-C15 was performed by using the gas chromatography-flam ionization detector (YL6500) supplemented with an HP-Ultra-2 column ( $250\text{ mm} \times 0.20\text{ mm} \times 0.11\text{ }\mu\text{m}$ ) according to the method described by Gao et al.<sup>1</sup>. A standard mixture composed of xylose, galactose, glucose, arabinose, and mannose monosaccharides was applied for the identification of monosaccharide profile.

#### *Fourier transform-infrared spectroscopy (FTIR)*

The analysis of the functional groups in the purified EPS-C15 was carried out by using an attenuated total reflectance (ATR-FTIR) spectrophotometer (Perkin-Elmer Inc., Norwalk, CT, USA) in the spectrum range of  $4000\text{--}400\text{ cm}^{-1}$  at room temperature. In addition, a diamond/ZnSe crystal plate was employed, and EPS-C15 powder was positioned on the plate.

#### *Nuclear magnetic resonance (NMR)*

The NMR analysis of EPS-C15 was performed by using an Avance III Bruker spectrometer (Bruker Corporation, MA, USA) equipped with a cryo-probe and z-axis gradient and operating at 600.19 and 150.92 MHz for  $^1\text{H}$  and  $^{13}\text{C}$ . All spectra were acquired at 298 K with a single sample prepared with 10 mg of product dissolved in 550  $\mu\text{L}$   $\text{D}_2\text{O}$  (Sigma). A general polysaccharide characterization procedure as reported by Bubb<sup>25</sup> was followed with one-dimensional (1D) and two-dimensional (2D) spectra ( $^1\text{H}$  and  $^{13}\text{C}$ ) used to determine the homonuclear and heteronuclear correlation pattern. Further experimental details are given in Supplementary Materials. The CASPER program ([www.casper.org.au/se/casper](http://www.casper.org.au/se/casper)) was applied to infer structural conclusions from the NMR as described by El-Deeb et al.<sup>26</sup>.

#### *Scanning electron microscopy (SEM)*

The surface morphology of EPS-C15 was assessed using scanning electron microscopy (SEM, Akishima, Tokyo, Japan) by operating at an accelerating voltage of 20 kV. The sample (5 mg) was air-dried and sputter-coated with gold using a Cressington 108 Auto Sputter Coater (Ted Pella Inc., Redding, CA, USA).

#### *Thermal properties*

A differential scanning calorimeter (DSC 25, TA instrument, DE, USA) was used to determine the thermal behavior of EPS-C15 under changes in temperature. An amount of 25 mg of EPS-C15 sample was heated in an alumina crucible from 20 to  $350\text{ }^{\circ}\text{C}$ , and an empty pan was applied as a reference. The thermogram was recorded following the protocol of Sasikumar et al.<sup>27</sup>. The DSC was repeated in triplicates.

#### *Zeta potential and particle size analysis*

Zeta potential is used to characterize the surface charge distribution and stability of EPSs. The Nano Plus Zeta potential and particle size analyzer (Particulate System, GA, USA) were utilized for the analysis of the zeta potential and particle size of EPS-C15 (0.5% w/v). The analysis was done as per the procedure reported by Sasikumar et al.<sup>27</sup>.

### Evaluation of EPS-C15 bioactivities

#### *Antioxidant capacity*

The ability of EPS-C15 to exert antioxidant activity was evaluated by in vitro ABTS and DPPH radical scavenging assays. For DPPH, 800  $\mu\text{L}$  of the DPPH reagent (0.1 mM DPPH dissolved in 95% methanol) was added to 200  $\mu\text{L}$  of EPS solution in glass test tubes. The mixture was shaken vigorously and incubated in the dark at room temperature for 30 min. Methanol was used as a blank. The absorbance of the incubated samples was measured at 517 nm<sup>28</sup>. For ABTS, a stock solution of ABTS was prepared by mixing stock solutions of 7.4 mM ABTS aqueous solution and 2.6 mM potassium persulphate aqueous solution in equal quantities (molar ratio = 1:0.35) and allowing them to react for 12 h in the dark at room temperature. A fresh ABTS reagent was prepared by mixing 1 mL of ABTS<sup>+</sup> solution with 50–60 mL of the buffered methanol to obtain an absorbance of  $0.70 \pm 0.02$  at 734 nm after equilibration at  $30\text{ }^{\circ}\text{C}$ . Twenty microliters of EPS solution was added to 2 mL of an ABTS reagent and incubated at  $30\text{ }^{\circ}\text{C}$  for 6 min. The absorbance of the mixture was measured at 734 nm<sup>28</sup>. The percentage of scavenging activity was assessed at two different concentrations of EPS-C15 (5 and 10 mg/mL) dissolved in dd-water<sup>9</sup>. The percentage of DPPH and ABTS scavenging activities was calculated using the following equation:

$$\text{Scavenging Rate(\%)} = \left[ 1 - \frac{A_{\text{sample}} - A_0}{A_{\text{control}} - A_0} \right] \times 100 \quad (1)$$

where  $A_0$  is the blank absorbance (negative control), and  $A_{\text{control}}$  refers to the absorbance of the radical (positive control).

#### Antidiabetic activity

Following the detailed procedure described by Ayyash et al.<sup>12</sup>, the inhibition of  $\alpha$ -amylase and  $\alpha$ -glucosidase was assessed by using two different concentrations (100 and 200  $\mu\text{g}$ ) of EPS-C15. The following equation was applied to calculate the inhibition percentages of  $\alpha$ -amylase and  $\alpha$ -glucosidase.

$$\text{Inhibition(\%)} = \left( 1 - \frac{\text{Abs}_{\text{sample}} - \text{Abs}_{\text{blank}}}{\text{Abs}_{\text{control}}} \right) \times 100 \quad (2)$$

#### Cytotoxic activity

Colon carcinoma (Caco-2) and breast carcinoma (MCF-7) cell lines were used to assess the cytotoxic activity of EPS-C15 at two concentrations (5 and 10 mg/mL). The protocol used was described in detail by Ayyash et al.<sup>9</sup>, and the percentage of cytotoxicity was calculated according to the following equation:

$$\text{Cytotoxicity(\%)} = \left[ 1 - \frac{R_{\text{sample}} - R_0}{R_{\text{control}} - R_0} \right] \times 100 \quad (3)$$

where  $R_{\text{sample}}$  is the absorbance ratio of OD570/OD605 of the EPS,  $R_{\text{control}}$  is the absorbance of the control sample (without EPS), and  $R_0$  is the average background considered a negative control with no cells.

#### Antibacterial activity

EPS-C15 was assayed for antibacterial activity against four foodborne pathogenic bacterial strains, including *S. aureus* ATCC 25923, *S. Typhimurium* 02-8423, *L. monocytogenes* ATCC 7644, and *E. coli* O157:H7. The experiment was performed by assessing the inhibition of bacteria as the EPS-C15 concentration increased following the detailed method described by Jeong et al.<sup>29</sup>. Briefly, 100  $\mu\text{L}$  of EPS-C15 aqueous solution (5 mg/mL) was added to the culture activated in brain heart infusion (250  $\mu\text{L}$ ), and then incubated for 18 h at 37 °C. Afterwards, the pathogens were enumerated on brain heart infusion agar and incubated for 24 h at 37 °C.

### Rheological properties

After the extraction of EPS-C15, the rheological tests were performed using a Discovery Hybrid Rheometer (TA Instruments, New Castle, DE, USA). Three aqueous solutions (5 mg/mL) of EPS-C15 were prepared by using 0.1 M of  $\text{CaCl}_2$ , 0.1 M of NaCl, and distilled-deionized water. In addition, the three solutions were prepared at two pH values (4.0 and 6.0). The rheological properties of the aqueous solutions were determined using cone and plate geometries (1 cone angle, 50 mm gap, and 50 mm diameter). The temperature of the plate was maintained at  $25.0 \pm 0.1$  °C.

#### Apparent viscosity

The flow curves of the extracted EPS-C15 solutions were measured upward and downward at a shear rate ranging from  $10^1$  to  $1000 \text{ s}^{-1}$ , with all the tests performed at  $25.0 \pm 0.1$  °C. The area between the upward and downward curves was used to evaluate the degree of thixotropy. In addition, the flow curves of EPS-C15 were described using the power law model (Eq. 4).

$$\tau = m \dot{\gamma}^\eta \quad (4)$$

where  $\tau$  is the shear stress,  $m$  is the consistency coefficient,  $\dot{\gamma}$  is the shear rate, and  $\eta$  is the flow behavior index.

#### Temperature-dependent behavior

The dependence of the apparent viscosity of EPS-C15 on temperature was assessed by raising the temperature up to 80 °C at a heating rate of 3 °C/min at a fixed shear rate of  $20 \text{ s}^{-1}$ . The flow activation energy of EPS-C15 was calculated by using Eq. 5 (Arrhenius equation).

$$n = n_0 e^{\frac{E_a}{RT}} \quad (5)$$

where  $n$  refers to the apparent viscosity,  $n_0$  is the Arrhenius constant,  $E_a$  is the flow activation energy,  $R$  is the gas constant, and  $T$  is the temperature in Kelvin.

#### Amplitude and frequency sweep tests

The amplitude test was performed to determine the linear viscoelastic region of EPS-C15. An amplitude strain sweep was carried out at a constant frequency of 1 Hz over a strain range of 0.1–20%. On the other hand, the frequency sweep test was conducted in the frequency range of 0.1–20 Hz at a constant strain within the linear viscoelastic region (<2%) to determine the viscoelastic behavior of EPS-C15, including the storage modulus

( $G'$ ), loss modulus ( $G''$ ), and the loss tangent ( $\tan \delta$ ). All amplitude and frequency sweep tests were carried out at a constant temperature of  $25.0 \pm 0.1$  °C.

#### Thixotropic behavior

Oscillation step tests were used to evaluate the breakdown of the inner structure of EPS-C15 under high shearing conditions and its subsequent recovery.  $G'$  and  $G''$  moduli were measured in an oscillation-time test at a frequency of 1.0 Hz with the following three test intervals: the first-time segment was 400 s at a stress of 0.2 Pa (to simulate behavior at rest within the linear viscoelastic range), the second segment was 60 s at a stress of 50 Pa (to simulate structural breakdown of EPS-C15 during application at high strain far beyond the linear viscoelastic range), and the third was 200 s at a stress of 0.2 Pa (to simulate structural regeneration at rest).

#### Statistical analysis

The different measurements were carried out in triplicate, and one-way analysis of variance (ANOVA) test was used to compare the differences. In addition, the quantitative data were expressed as mean  $\pm$  standard deviation with  $P < 0.05$  considered statistically significant. Moreover, Fisher's test was applied to compare mean values at the level of significance.

## Results and discussion

### Molecular weight and monosaccharide composition of EPS-C15

EPSs chemical composition varies between species and strains, which, by the way, influences their properties and potential applications<sup>6</sup>. The results obtained by gel permeation chromatography and refractive index analysis showed that the partially purified EPS-C15 had an average molecular weight of  $8.8 \times 10^5$  Da (Fig. S1), which was higher than the molecular weight of the EPS partially purified from *L. bulgaricus* ( $5.37 \times 10^4$  Da)<sup>11</sup>. It was reported that the molecular weight of LAB-EPSs was in the range between 123.84 and 178.72 kDa<sup>30</sup>. According to the chemical composition, EPSs produced by *L. lactis* strains can be classified as neutral or acidic. Neutral EPSs are composed of two or more different monosaccharide units, but neither organic acids nor acidic EPSs present uronic acid groups. The monosaccharide composition analysis revealed that EPS-C15 is composed of arabinose, xylose, mannose, and glucose at a molar ratio of 2.0:2.7:1.0:21.3, respectively (Table S1). EPS produced by *L. lactis* IMAU11823 comprised glucose and mannose with a molar ratio of 7.01:1.00, and a molecular weight of  $6.10 \times 10^5$  Da, while another EPS produced by the same strain was composed of mannose, glucose, and rhamnose at molar ratios of 7.45:1.00:2.34, and a molecular weight of  $2.93 \times 10^5$  Da<sup>31</sup>. Furthermore, it was reported that ribose, fucose, mannose, glucose, galactose, and arabinose with a molar ratio of 5.48:0.39:9.77:4.03:1.00:1.92, respectively were the main monosaccharides of an EPS extracted from *L. lactis*<sup>32</sup>. Another study reported that mannose, ribose, rhamnose, glucuronic acid, glucose, galactose, xylose, and arabinose, representing 3.97, 4.83, 3.59, 6.83, 44.10, 23.91, 6.34, and 6.43, respectively, were the predominant monosaccharides in the EPS produced from *L. lactis*<sup>30</sup>. Glucose, which positively affects the viscosity of EPSs, is commonly found in their monosaccharide composition. Moreover, the presence of galactose, glucuronic acid, mannose, arabinose, rhamnose, fucose, xylose, and fructose in EPSs has been reported<sup>33</sup>.

### FTIR and NMR

The infrared spectrum of the functional group analysis obtained by the ATR-FTIR is elucidated in Fig. 1. It was shown that the absorption bands at  $843.63$   $\text{cm}^{-1}$  and  $916.72$   $\text{cm}^{-1}$  could be assigned to the  $\alpha$ - and  $\beta$ -configurations of the sugar units<sup>34</sup>. In addition, the band at  $3302.18$   $\text{cm}^{-1}$  was the ideal stretching vibration of the hydroxyl group. The elongating vibration of the C–H (asymmetrical) of the aliphatic  $\text{CH}_2$  group was assigned to  $2925.51$   $\text{cm}^{-1}$ <sup>35</sup>. The  $1646.74$   $\text{cm}^{-1}$  band was attributed to the stretching vibration of a carboxyl group<sup>36</sup>. Furthermore, the region of  $900$ – $1200$   $\text{cm}^{-1}$  was attributed to the vibrations of the C–O–C glycosidic linkages. This region is described as the fingerprint of EPSs<sup>34</sup>. The band at  $1414.78$   $\text{cm}^{-1}$  was ascribed to the bending vibrations of the O–H bond. It is worth noting that the absence of  $1730$  and  $1720$   $\text{cm}^{-1}$  bands implies that EPS-C15 does not encompass uronic acid<sup>37,38</sup>.

Figure 2 groups the NMR evidence obtained for EPS-C15, namely the 1D  $^1\text{H}$  (panel A),  $^{13}\text{C}$  (panel B) traces, and the 2D  $^{13}\text{C}$ - $^1\text{H}$  HSQC (panel C), 2D  $^1\text{H}$ - $^1\text{H}$  TOCSY (panel D) maps. An overlay of 2D  $^{13}\text{C}$ - $^1\text{H}$  HMBC and 2D  $^{13}\text{C}$ - $^1\text{H}$  HSQC is also shown (Fig. 2E). The peaks occurring in the region from 3 to 4 ppm in the  $^1\text{H}$  NMR spectrum arise from the sugar protons H-2, H-3, H-4, H-5, and H-6. The anomeric proton and carbon resonances typically occur in the regions 4.7–5.5 ppm of  $^1\text{H}$  spectra and 95.0–110.0 ppm of  $^{13}\text{C}$  spectra, respectively<sup>35</sup>. Assignments were carried out based on the connectivity pattern that could be established from the analysis of the TOCSY and HSQC maps. The consistency of the interpretation was further controlled by comparing the long-range relayed correlation of the HMBC map to the corresponding HSQC and TOCSY connectivities (Fig. 2E). The experimental information was then matched with the CASPER software<sup>39</sup> computation to obtain identification and configuration of the polysaccharide units. The pattern of  $\alpha$ -configurations of D-glucopyranose and D-xylopyranose and  $\beta$ -configurations of D-mannopyranose could be assessed. The CASPER attribution of the experimental anomeric CH correlations obtained from  $^1\text{H}$ - $^{13}\text{C}$  NMR HSQC is presented in Table 1. Based on the computation results, the proposed backbone structure of EPS-C15 is:  $\rightarrow 3)\alpha\text{-d-Glc}^{\text{vi}}(1 \rightarrow 3)\alpha\text{-d-Xyl}^{\text{v}}(1 \rightarrow 6)\alpha\text{-d-Glc}^{\text{iv}}(1 \rightarrow 4)\alpha\text{-d-Glc}^{\text{iii}}(1 \rightarrow 3)\beta\text{-d-Man}^{\text{ii}}(1 \rightarrow 2)\alpha\text{-d-Glc}^{\text{c}}(1 \rightarrow )$ . It is assumed that arabinose is attached to the terminals<sup>37</sup>. The  $^{13}\text{C}$  NMR spectrum did not exhibit any peak at  $\delta > 170$  ppm, which denotes the lack of uronic acid function<sup>37</sup>.

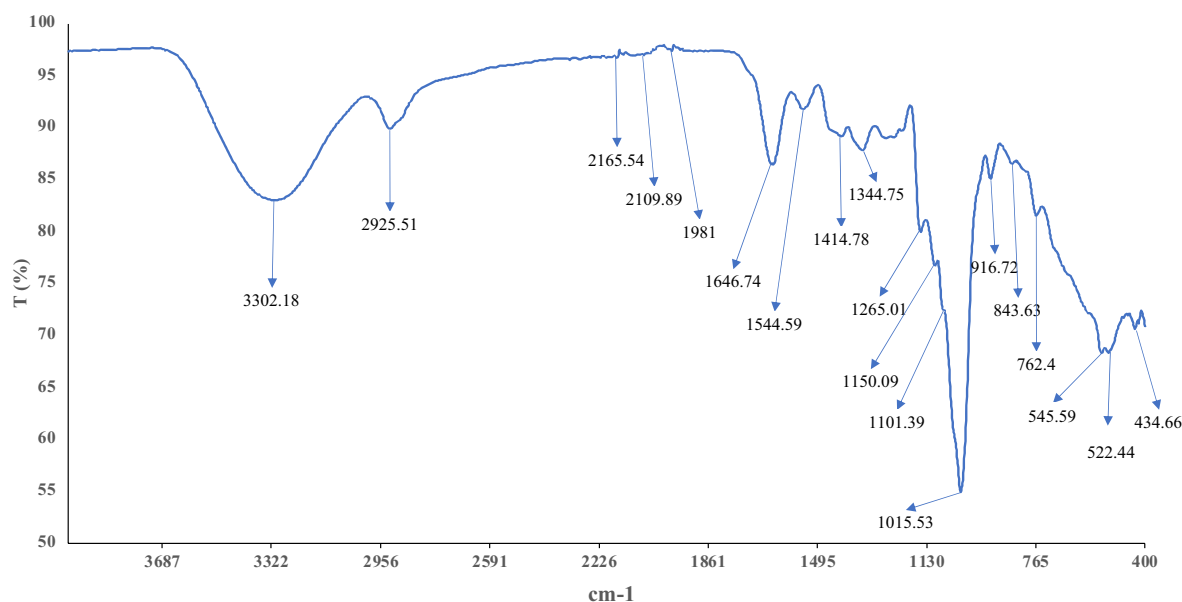


**Figure 1.** FTIR spectrum of EPS-C15 at wavenumbers range of 4000–400  $\text{cm}^{-1}$ .

## SEM, thermal properties, zeta potential, and particle size

### SEM and thermal properties

The microstructure morphology of EPS-C15 at different magnifications is shown in Fig. 3A,B. The SEM image exhibited a porous structure of EPS-C15 and a flake-like basic configuration. A similar structure was observed for the EPS extracted from the bacterial strain *L. lactis* F-mou isolated from Sahrawi camel milk<sup>33</sup>. The porous network is commonly attributed to *L. lactis* colonies and may contribute to the retained extra moisture, which is a beneficial characteristic for food production, such as cheese-making<sup>34</sup>. The thermal behavior of EPS-C15 analyzed by the DSC (Fig. 3C) exhibited two endothermic peaks and one exothermic peak. The thermal analysis demonstrated that EPS-C15 exhibited two endothermic peaks at 58.43 °C accredited to the glass transition ( $T_g$ ) and 159.68 °C corresponding to the melting point ( $T_m$ ). The degradation of EPS-C15 occurred at 265.62 °C, represented by the exothermic peak. The higher values of  $T_g$  and  $T_m$  suggested that EPS-C15 was stable at elevated temperatures, indicating an advantage to thermal processes in the food processing industries.

### Zeta potential and particle size

The values of zeta potential and particle size of EPS-C15 were  $-12.44$  mV and 311.2 nm, respectively. The zeta potential value predicts the colloidal suspension stability of a solution. For better physical colloidal stability, an adequate zeta potential value ranges between  $-30$  and  $30$  mV<sup>34</sup>. It was reported that the average zeta potential of two EPSs secreted by the *L. lactis* IMAU11823 strain represented  $-3.26$  mV and  $-9.10$  mV, respectively. The two EPSs exhibited diverse particle size distributions. The first EPS showed a single and uneven particle size distribution, mostly in the range between 100 and 1000 nm. The second EPS was mainly distributed in the range of 15–50 nm and 3000–7000 nm, characterized by two comparatively narrow but even peaks. Overall, higher zeta potential values are associated with better solution stability. Accordingly, the variations in zeta potential and particle size distribution among EPSs from different LAB suggested clear variations in their chemical and physical nature<sup>31</sup>.

## Bioactive properties of EPS-C15

### Antioxidant capacity

The EPS-C15 produced by *L. lactis* C15 showed a potent antioxidant capacity. The results revealed that at 5 mg/mL and 10 mg/mL of EPS-C15, DPPH results were 41.8% and 22.5%, respectively, and the ABTS results represented 50.3% and 46.4%, respectively (Fig. 4). The antioxidant activities were elevated by increasing the level of crude EPS from *L. lactis* IMAU11823, implying a dose-dependent correlation<sup>31</sup>. It was reported that polysaccharides derived from *L. lactis* exhibited antioxidant capacities, which can scavenge DPPH radicals, hydroxyl radicals,  $\text{H}_2\text{O}_2$ , peroxy radicals, superoxide radicals, alkyl radicals, ABTS radicals, and exhibit a reducing power. The composition and the molar ratio of monosaccharides, as well as the types of the glycosyl linkages are crucial in articulating the antioxidant properties of EPSs<sup>1</sup>. Glucose 1  $\rightarrow$  6 and arabinose 1  $\rightarrow$  4 were closely related to DPPH radical scavenging effect<sup>40</sup>. The antioxidant capacity of EPSs appears to correlate with the monosaccharide's composition. This is in consonance with the results of Al-Nabulsi et al.<sup>11</sup> documenting the antioxidant capacity of EPS-L secreted by *L. bulgaricus* from labneh. The antioxidant activities of biomolecules depend on their chemical and physical structure; hence, it would be required to explain the antioxidant activity of biomolecules according to their structural properties. Moreover, monosaccharides profile and functional groups are the main key factors for the antioxidant activity of EPSs<sup>14</sup>.

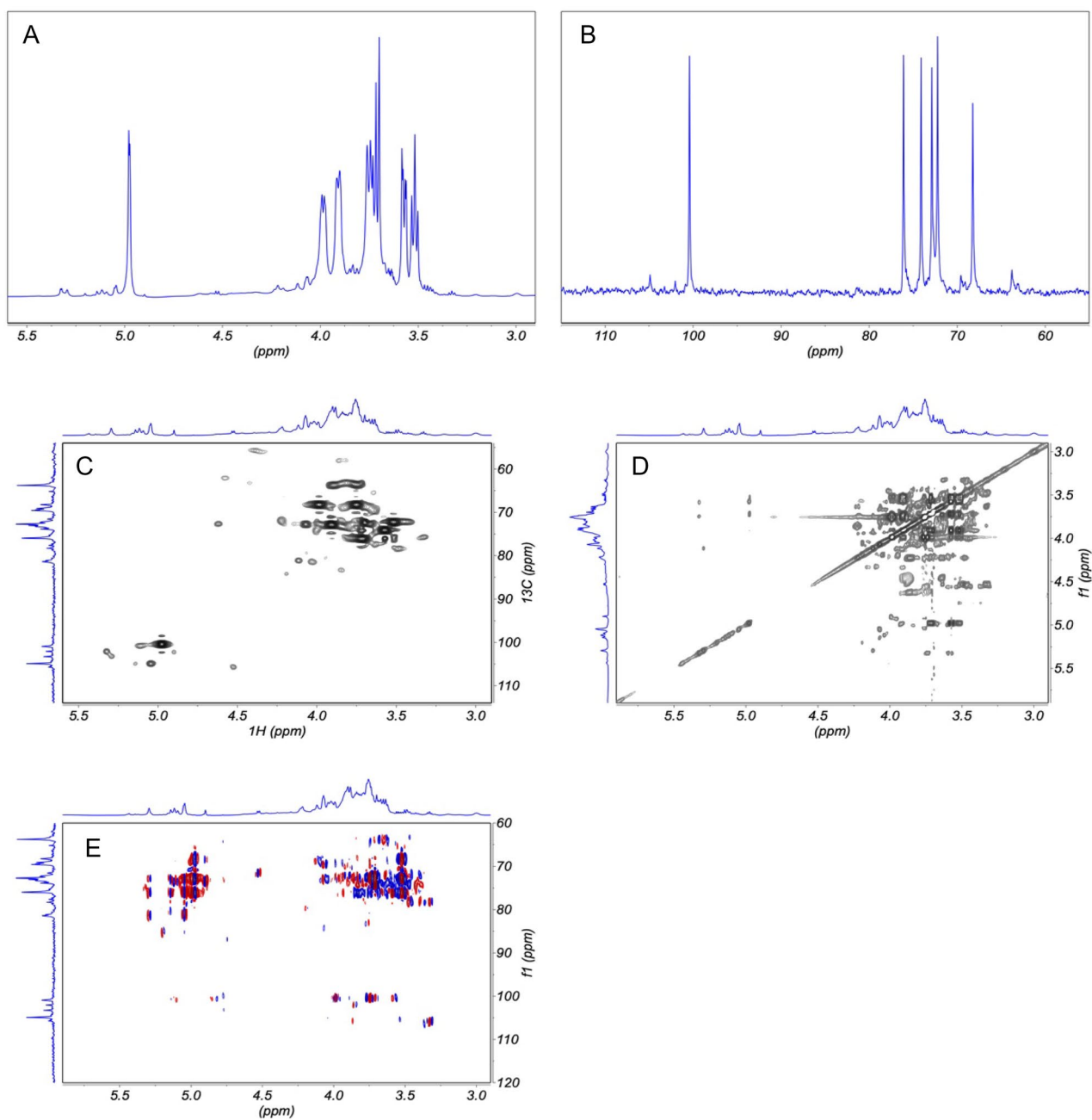


**Figure 2.** 1D and 2D NMR analysis of EPS-C15. (A) Region from 1D  $^1\text{H}$  spectrum. (B) Region from 1D  $^{13}\text{C}$  spectrum. (C) Region from 2D  $^1\text{H}$  TOCSY. (D) Region from 2D  $^{13}\text{C}$ - $^1\text{H}$  HSQC spectrum. (E) Overlay of 2D  $^{13}\text{C}$ - $^1\text{H}$  HSQC (black contours) and 2D  $^{13}\text{C}$ - $^1\text{H}$  HMBC (red-blue contours).

EPS partially purified from M-17 broth culture of *L. lactis* isolated from milk sources showed strong DPPH capacities at different doses (5–7.5 mg/mL), and it was observed that the extracted EPS exhibited a dose-dependent scavenging capacity. In addition, *L. lactis* F-mou EPS isolated from Sahrawi camel milk exhibited DPPH scavenging capacities at all assayed concentrations (1–4 mg/mL), and as observed, the antioxidant efficiency was EPS dose-dependent<sup>33</sup>. It was reported that the EPS secreted by *L. lactis* NCR112 isolated from *Phyllanthus urinaria* showed a DPPH scavenging capacity of 52.86% at 10 mg/mL<sup>41</sup>. It was also observed that the EPS produced by *L. lactis* 12 isolated from Chinese pickled cabbage displayed in vitro scavenge abilities against hydroxyl and superoxide anion radicals and significantly reduced the malondialdehyde level, while raising the activity of catalase and superoxide dismutase in mice in a dose-dependent manner<sup>42</sup>.

#### Antidiabetic activity

The results show that EPS-C15 demonstrated strong  $\alpha$ -amylase and  $\alpha$ -glucosidase inhibitory activities (Fig. 4). The inhibition of  $\alpha$ -amylase represented 88 and 89.3%, while  $\alpha$ -glucosidase inhibition was 87.2 and 85% at a

Residues	NMR	Chemical shifts (ppm) <sup>a</sup>					
		1	2	3	4	5	6,6'
→2)α-d-Glc <sup>i</sup> (1→	<sup>1</sup> H	111.86	82.53	76.99	70.45	85.32	61.47
	<sup>13</sup> C	5.57	3.95	4.11	3.50	4.48	3.83,4.00
→3)β-d-Man <sup>ii</sup> (1→	<sup>1</sup> H	103.13	95.28	83.20	n.d	78.26	63.07
	<sup>13</sup> C	4.98	4.64	3.84	3.97	3.57	3.98,4.08
→4)α-d-Glc <sup>iii</sup> (1→	<sup>1</sup> H	104.85	75.96	87.44	79.91	102.89	61.56
	<sup>13</sup> C	5.18	3.93	4.66	3.72	4.45	3.99,4.06
→6)α-d-Glc <sup>iv</sup> (1→	<sup>1</sup> H	102.26	76.68	77.74	69.57	88.89	68.23
	<sup>13</sup> C	5.32	3.95	4.03	3.53	4.43	3.90,3.98
→3)α-d-Xyl <sup>v</sup> (1→	<sup>1</sup> H	100.40	72.22	105.74	69.09	63.79	ND
	<sup>13</sup> C	5.14	3.65	4.18	4.04	3.59	3.61
→3)α-d-Glc <sup>vi</sup> (1→	<sup>1</sup> H	104.91	84.23	85.38	70.56	84.42	61.28
	<sup>13</sup> C	5.29	4.19	4.06	3.72	4.57	3.92,4.02

**Table 1.** <sup>1</sup>H and <sup>13</sup>C chemical shift assignments of EPS-C15. <sup>a</sup>Chemical shift assignment by CASPER.

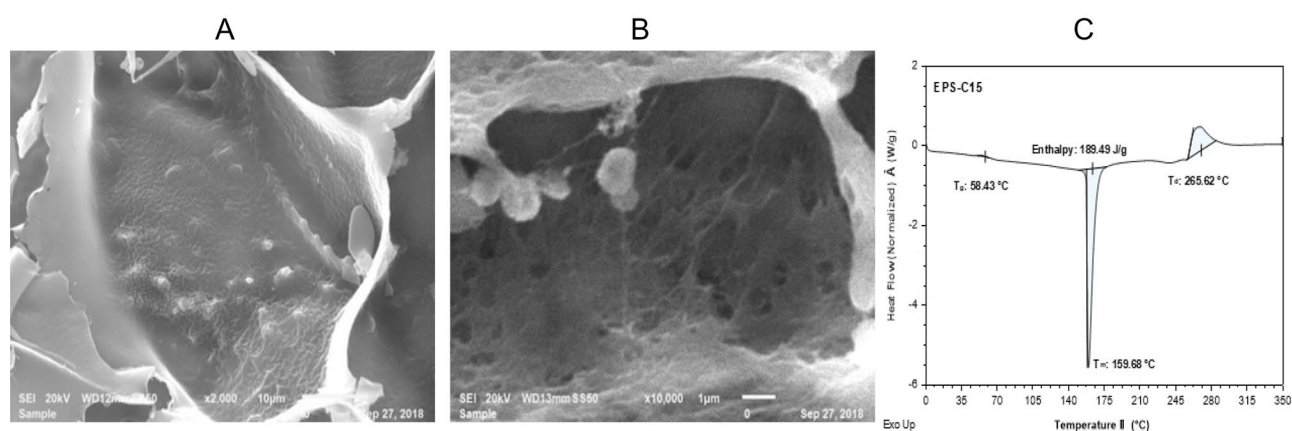


**Figure 3.** SEM images at magnifications 1000×(A) and 1800×(B) and DSC thermogram (C) of EPS-C15.

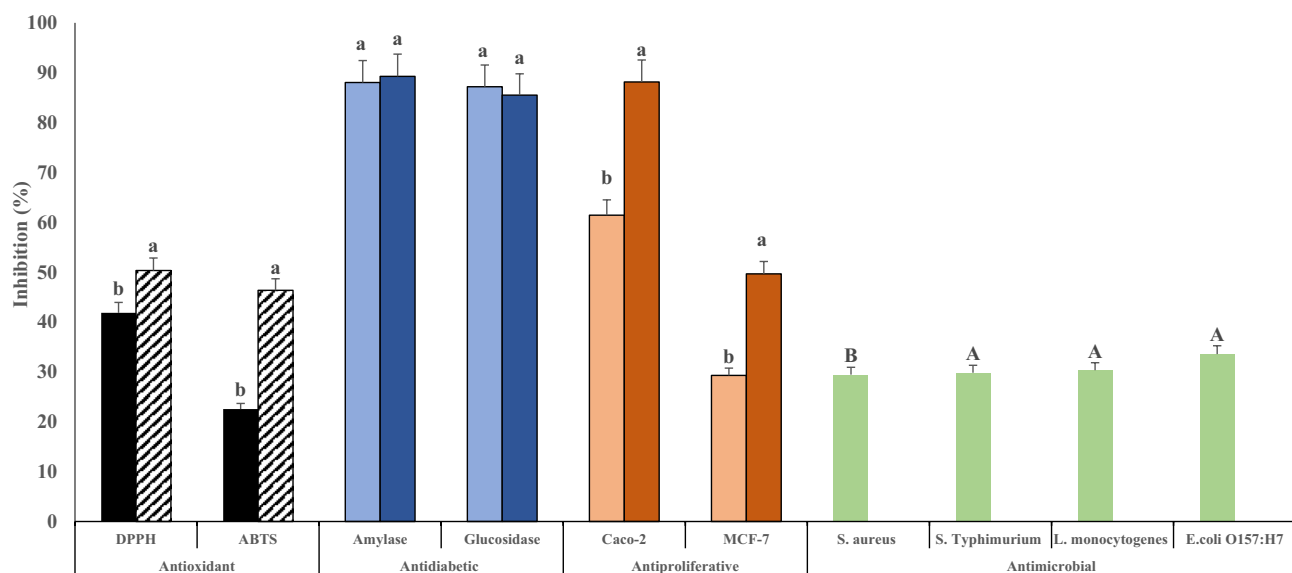


**Figure 4.** Bioactivities of EPS-C15. Antioxidant [5 mg (black square) and 10 mg (striped square)], antidiabetic [100 μg (light blue square) and 200 μg (dark blue square)], antiproliferative activities [5 mg (orange square) and 10 mg (brown square)], and antibacterial activities [5 mg/mL (green square)]. Bars are means ± standard deviation (n=6).



concentration of 100 and 200  $\mu\text{g}$  of EPS-C15, respectively. Glucosidase inhibitors play an important role in diabetes management, and they have been used in the suppression of post-prandial glucose levels in diabetic patients. These inhibitors are widely distributed in living organisms and act by inhibiting enzymes involved in glucose metabolism, leading to a reduction in starch hydrolysis. *L. lactis* antidiabetic effects have been tested, but so far, the inhibitory effects of the EPS secreted by *L. lactis* against  $\alpha$ -amylase and  $\alpha$ -glucosidase activities have not been described<sup>28</sup>.

#### Antiproliferative activity

The effects of probiotics on different types of cancer cell lines have been reported<sup>43</sup>. Polysaccharides can act as anticancer agents through a broad spectrum of cellular mechanisms, and it was frequently observed that the antiproliferative effects were attributed to the presence of probiotics. As shown in Fig. 4, the concentrations of 5 and 10 mg of EPS-C15 were tested against Caco-2 (human epithelial colorectal adenocarcinoma) and MCF-7 (human breast cancer) cell lines. The results show that the antiproliferative effect against Caco-2 and MCF-7 cell lines, respectively, represented 61.4% and 29.3% of inhibition with 5 mg of EPS, and 88.1% and 49.7% inhibition with 10 mg of EPS. It was reported that the EPS derived from *L. lactis* subsp. *lactis* demonstrated antiproliferative effects by triggering cellular mechanisms leading to cell death in MCF-7 cells<sup>32</sup>. Similarly, 10 mg/mL of the EPS secreted by *L. lactis* NCR112 isolated from *P. urinaria* expressed 86.86% and 50.36% cytotoxic effects against HeLa and HepG2 cell lines, respectively<sup>41</sup>.

#### Antimicrobial activity

EPSs have been stated to comprise different functional groups, such as phosphate, hydroxyl, and carbonyl groups, which were proposed to act a vital role in delivering antimicrobial features<sup>44</sup>. EPS-C15 displayed a significant antimicrobial behavior against all the tested foodborne pathogens (Fig. 4). Among the tested pathogenic bacteria, the extracted EPS showed the highest bactericidal effect against *E. coli* O157:H7 (33.6%), followed by *L. monocytogenes* (30.3%), *S. Typhimurium* (29.8%), and *S. aureus* (29.5%). EPS-C15 had the least significant effect ( $p < 0.05$ ) on *S. aureus*, which could be attributed to the bacteria's resistance to EPS. Antimicrobial effects were also observed in the EPS produced by *L. lactis* F-mou strain, which possessed a great inhibition against the gram-positive bacteria<sup>33</sup>. EPSs could promote secondary metabolites aggregation in the growth media, which might negatively influence pathogens' growth<sup>45</sup>. Furthermore, EPS can sequester essential nutrients required for microbial growth, thereby limiting the proliferation of potential pathogens. Additionally, some EPS possess direct antimicrobial properties, often attributed to their unique structural characteristics and charge distributions, which can disrupt microbial cell membranes or interfere with essential cellular processes. In addition, EPS could break down the genetic materials (DNA and RNA) inside pathogenic cells<sup>46</sup>. Similarly, the functional groups present in EPSs structure might interact with the microbial cell membranes, yielding antimicrobial actions<sup>14</sup>.

### Rheological properties

#### Apparent viscosity and flow curves of EPS-C15

The dependence of the apparent viscosity of EPS-C15 on the shear rate is presented in Fig. 5A. It is evident that EPS-C15 solutions showed higher viscosity, especially at low shear rates. The addition of NaCl or CaCl<sub>2</sub> to EPS-C15 solutions caused a reduction in the apparent viscosity. The lowest viscosity of EPS-C15 was recorded in acidic salt solutions (pH 4.0). This finding implies that the two cations (Ca<sup>2+</sup> and Na<sup>+</sup>) might have adverse effects on the viscosity of the EPS-C15-containing product. The decrease in EPS-C15 viscosity can be attributed to the screening effect of the electrolyte on the inter-molecular H-bonding, which might cause a decrease in the three-dimensional network strength<sup>47</sup>. Moreover, the intra-molecular electrostatic repulsions among negatively charged groups in EPS-C15 molecules can contribute to this viscosity reduction by curling polymer coils<sup>47</sup>.

On the other hand, the effect of pH on the viscosity was more pronounced than the effect of salt types, as EPS solutions at pH 6.0 showed higher viscosity than the solutions adjusted at pH 4.0, which can be attributed to the increase of the ionization degree of carboxyl groups in polysaccharide molecules with increasing pH value. This finding agrees with those of Li et al.<sup>48</sup>, who reported higher viscosity of EPS-POS16 at pH 6.0 to 9.0. The decrease in the viscosity of EPS-C15 solutions with increasing electrolyte concentration has been reported for a number of EPSs<sup>48</sup>. It should also be mentioned that the viscosity of EPS-C15 displayed a similar apparent viscosity behavior to other EPSs studied under the same conditions, such as EPS-C47<sup>7</sup>.

Figure S2 shows that all EPS-C15 solutions exhibited a shear thinning behavior as the apparent viscosity decreased with the shear rate. The flow behavior index values obtained from fitting the flow curves with the Power law model (Fig. S2, Table S2) demonstrated that EPS-C15 in water had the highest deviation from Newtonian behavior ( $\eta = 1$ ). In contrast, the lowest deviation was detected in samples in electrolyte solutions at pH 6.0. It should be noted that the area of hysteresis loops formed from the upward and downward flow curves was very small for all samples within the experimental errors. This indicates that EPS-C15 exhibited a time-independent behavior under the conditions of the rheological property measurements.

Figure 5B shows the dependence of the apparent viscosity of EPS-C15 on temperature. At a low temperature ( $25 \pm 0.1$  °C), the apparent viscosity of EPS-C15 in CaCl<sub>2</sub> solution at pH = 6.0 was the highest, followed by the same solution at pH 4.0. However, the apparent viscosity of both samples decreased at a temperature higher than 40 °C. This resulted from the effect of the thermal energy on the weak intermolecular forces between EPS-C15 molecules. The differences in the apparent viscosity of different EPS-C15 solutions could not be discerned at temperatures greater than 40 °C. Furthermore, the activation energy of flow presented in Table S3 and determined by Arrhenius' equation ranged from 10.1 to 33.7 kJ/mol. The highest and lowest activation energy was observed in EPS-C15 in CaCl<sub>2</sub> solution (pH 4.0) and water (pH 6.0), respectively. Overall, the pH did not show significant influences on the activation energy.

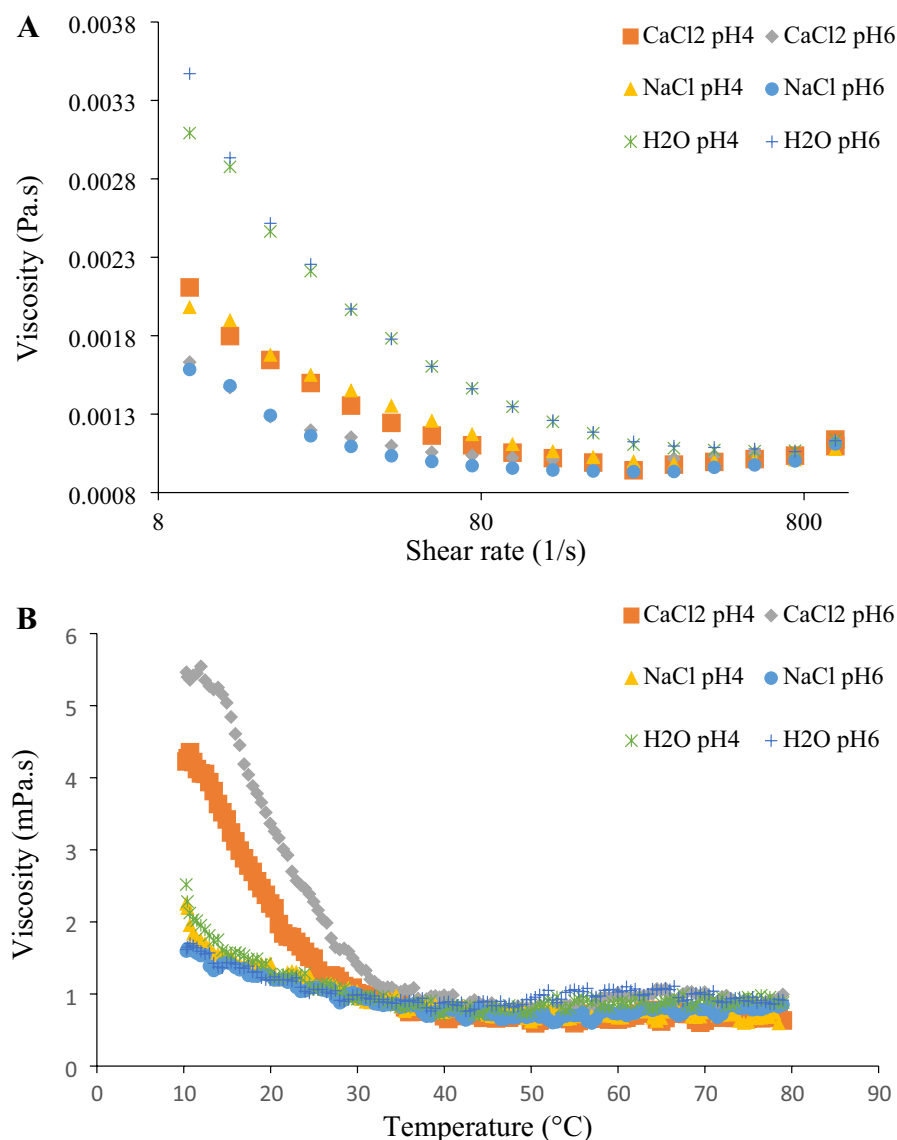


**Figure 5.** Apparent viscosity (**A**) and temperature-dependent viscosity behavior (**B**) of EPS-C15 in CaCl<sub>2</sub> at pH 6.0 (diagonal), CaCl<sub>2</sub> at pH 4.0 (square), NaCl at pH 6.0 (circle), NaCl at pH 4.0 (triangle), H<sub>2</sub>O at pH 6.0 (+), H<sub>2</sub>O at pH 4.0 (times symbol). The tests were repeated in duplicates.

#### Viscoelastic behavior of EPS-C15

The amplitude sweep test was conducted to determine the limit of the linear viscoelastic region for EPS-C15. As shown in Fig. S3 (a and b), the linearity limit for  $G'$  and  $G''$  moduli of all EPS-C15 solutions was less than 2.0% strain. Therefore, the frequency sweep tests of EPS-C15 were carried out at 0.8% strain to avoid mutilation of the structure of the sample during the test. As evident in Fig. S4, the viscous behavior of EPS-C15 solutions was dominant over the elastic behavior at a frequency less than 3.0 Hz. EPS-C15 in CaCl<sub>2</sub> solution at pH 4.0 was an exception, where the elastic modulus was more significant than the viscous modulus over the entire frequency range tested. The same sample showed the highest values for both elastic and viscous moduli. Moreover,  $G'$  and  $G''$  of this sample were relatively independent of frequency, opposing the behavior of most EPS-C15 solutions, where both moduli increased with frequency. This behavior can be attributed to the cross-linking effects of cations ( $\text{Ca}^{2+}$ ) with the carboxyl groups in EPS-C15.

#### Thixotropic behavior of EPS-C15

In addition to the flow curves hysteresis test, the oscillation step test was performed to evaluate the thixotropic behavior of EPS-C15 solutions. Figure S5 reveals that all EPS-C15 solutions exhibited a time-dependent behavior, as  $G'$  and  $G''$  moduli values returned back approximately to their original values after releasing the high stress applied. This indicates that the rate of rebuilding the structure in EPS-C15 samples was equivalent to the rate of structure breaking upon the shearing process. Overall, EPS-C15 recovery rates were not affected by the

addition of salts. The results of the oscillation step test were in consonance with the flow curves hysteresis test. These findings agree with the rheological properties reported for the EPSs secreted by *Porphyridium sordidum* and *Porphyridium purpureum* in mono and divalent salt solutions<sup>49</sup>.

## Conclusions

An exopolysaccharide (EPS-C15) was biosynthesized by *L. lactis* C15. The partially purified EPS-C15 was characterized by FTIR, NMR, and SEM techniques and examined for its physicochemical, biological, and rheological properties. The structural analysis revealed that EPS-C15 was mainly composed of  $\alpha$ -1,3 and  $\alpha$ -1,6 linked D-glucopyranose units with an average molecular weight of  $8.8 \times 10^5$  Da. The porous network structure, which is specific to EPS from *L. lactis*, and its excellent rheological properties strongly support the potential use of EPS-C15 in the food and pharmaceutical industries. EPS-C15 exhibited radical scavenging activities against DPPH (41.8 and 50.3%) and ABTS (22.5 and 46.4%) at 5 and 10 mg/mL, respectively. The antiproliferative activity increased by increasing the concentration of EPS-C15 from 5 to 10 mg, representing 61.4 and 88.1% against Caco-2 and 29.3 and 49.7% against MCF-7, respectively. Furthermore, the type of salt and variations in pH values significantly influenced the rheological characteristics of EPS-C15. EPS-C15 exhibited significant biological activities, including antibacterial, antioxidant, antitumor, and antidiabetic activities, and was highly thermally stable. Therefore, EPS-C15 could be considered a potential biomaterial in the healthcare industry and in thermal processing in the food industry. Further investigation, which may include extensive clinical trials, is required to verify the purported health benefits of EPS-C15. It would be highly advantageous to explore the effects of EPS in realistic scenarios, such as food matrices.

## Data availability

All data generated or analysed during this study are included in this published article and its supplementary information files.

Received: 11 July 2023; Accepted: 11 October 2023

Published online: 19 October 2023

## References

- Gao, Z. *et al.* Antioxidant and anti-inflammatory properties of an aminoglycan-rich exopolysaccharide from the submerged fermentation of *Bacillus thuringiensis*. *Int. J. Biol. Macromol.* **220**, 1010–1020 (2022).
- Rana, S. & Upadhyay, L. S. B. Microbial exopolysaccharides: Synthesis pathways, types and their commercial applications. *Int. J. Biol. Macromol.* **157**, 577–583 (2020).
- Saadat, Y. R., Khosroushahi, A. Y. & Gargari, B. P. A comprehensive review of anticancer, immunomodulatory and health beneficial effects of the lactic acid bacteria exopolysaccharides. *Carbohydr Polym.* **217**, 79–89 (2019).
- Jurášková, D., Ribeiro, S. C. & Silva, C. C. Exopolysaccharides produced by lactic acid bacteria: From biosynthesis to health-promoting properties. *Foods* **11**(2), 156 (2022).
- Ruas-Madiedo, P. & De Los Reyes-Gavilán, C. Invited review: Methods for the screening, isolation, and characterization of exopolysaccharides produced by lactic acid bacteria. *J. Dairy Sci.* **88**(3), 843–856 (2005).
- Zhou, Y., Cui, Y., Suo, C., Wang, Q. & Qu, X. Structure, physicochemical characterization, and antioxidant activity of the highly arabinose-branched exopolysaccharide EPS-M2 from *Streptococcus thermophilus* CS6. *Int. J. Biol. Macromol.* **192**, 716–727 (2021).
- Ayyash, M. *et al.* Exopolysaccharide produced by the potential probiotic *Lactococcus garvieae* C47: Structural characteristics, rheological properties, bioactivities and impact on fermented camel milk. *Food Chem.* **333**, 127418 (2020).
- Ayyash, M., Olaimat, A., Al-Nabulsi, A. & Liu, S.-Q. Bioactive properties of novel probiotic *Lactococcus lactis* fermented camel sausages: Cytotoxicity, angiotensin converting enzyme inhibition, antioxidant capacity, and antidiabetic activity. *Food Sci. Anim. Resour.* **40**(2), 155 (2020).
- Ayyash, M. *et al.* Physicochemical, bioactive and rheological properties of an exopolysaccharide produced by a probiotic *Pediococcus pentosaceus* M41. *Carbohydr. Polym.* **229**, 115462 (2020).
- Ayoub, N. M., Alkhalifa, A. E., Ibrahim, D. R. & Alhusban, A. Combined crizotinib and endocrine drugs inhibit proliferation, migration, and colony formation of breast cancer cells via downregulation of MET and estrogen receptor. *Med. Oncol.* **38**(1), 8 (2021).
- Al-Nabulsi, A. A. *et al.* Characterization and bioactive properties of exopolysaccharides produced by *Streptococcus thermophilus* and *Lactobacillus bulgaricus* isolated from labaneh. *LWT* **167**, 113817 (2022).
- Ayyash, M. *et al.* Characterization, bioactivities, and rheological properties of exopolysaccharide produced by novel probiotic *Lactobacillus plantarum* C70 isolated from camel milk. *Int. J. Biol. Macromol.* **144**, 938–946 (2020).
- Huang, Z. *et al.* An exopolysaccharide from *Lactobacillus plantarum* H31 in pickled cabbage inhibits pancreas  $\alpha$ -amylase and regulating metabolic markers in HepG2 cells by AMPK/PI3K/Akt pathway. *Int. J. Biol. Macromol.* **143**, 775–784 (2020).
- Zhou, Y., Cui, Y. & Qu, X. Exopolysaccharides of lactic acid bacteria: Structure, bioactivity and associations: A review. *Carbohydr. Polym.* **207**, 317–332 (2019).
- Jiang, B. *et al.* Separation, structural characteristics and biological activity of lactic acid bacteria exopolysaccharides separated by aqueous two-phase system. *Lwt* **147**, 111617 (2021).
- Wu, J., Zhang, Y., Ye, L. & Wang, C. The anti-cancer effects and mechanisms of lactic acid bacteria exopolysaccharides in vitro: A review. *Carbohydr. Polym.* **253**, 117308 (2021).
- Bukvicki, D. *et al.* Unravelling the potential of *Lactococcus lactis* strains to be used in cheesemaking production as biocontrol agents. *Foods* **9**(12), 1815 (2020).
- Surber, G. *et al.* Cream cheese made with exopolysaccharide-producing *Lactococcus lactis*: Impact of strain and curd homogenization pressure on texture and syneresis. *J. Food Eng.* **308**, 110664 (2021).
- Feng, J. *et al.* Effects of an exopolysaccharide from *Lactococcus lactis* Q-9 on innate immune response, antioxidant activity, and disease resistance against *Aeromonas hydrophila* in *Cyprinus carpio*. *J. Fish. China* **44**(9), 1477–1487 (2020).
- Feng, J. *et al.* Effects of an exopolysaccharide from *Lactococcus lactis* Z-2 on innate immune response, antioxidant activity, and disease resistance against *Aeromonas hydrophila* in *Cyprinus carpio* L. *Fish Shellfish Immunol.* **98**, 324–333 (2020).
- Kleerebezem, M. *et al.* Exopolysaccharides produced by *Lactococcus lactis*: From genetic engineering to improved rheological properties? In *Lactic Acid Bacteria: Genetics, Metabolism and Applications: Proceedings of the Sixth Symposium on lactic acid bacteria: genetics, metabolism and applications, 19–23 September 1999, Veldhoven, The Netherlands* (eds Konings, W. N. *et al.*) 357–365 (Dordrecht, Springer, 1999).

22. Abushelaibi, A., Al-Mahadin, S., El-Tarabily, K., Shah, N. P. & Ayyash, M. Characterization of potential probiotic lactic acid bacteria isolated from camel milk. *LWT Food Sci. Technol.* **79**, 316–325 (2017).
23. Wang, J., Wu, T., Fang, X., Min, W. & Yang, Z. Characterization and immunomodulatory activity of an exopolysaccharide produced by *Lactobacillus plantarum* JLK0142 isolated from fermented dairy tofu. *Int. J. Biol. Macromol.* **115**, 985–993 (2018).
24. Kansandee, W., Moonmangmee, D., Moonmangmee, S. & Itsaranuwat, P. Characterization and *Bifidobacterium* sp. growth stimulation of exopolysaccharide produced by *Enterococcus faecalis* EJR152 isolated from human breast milk. *Carbohydr. Polym.* **206**, 102–109 (2019).
25. Bubb, W. A. NMR spectroscopy in the study of carbohydrates: Characterizing the structural complexity. *Concept Magn. Reson. A* **19**(1), 1–19 (2003).
26. El-Deeb, N. M., Yassin, A. M., Al-Madboly, L. A. & El-Hawiet, A. A novel purified *Lactobacillus acidophilus* 20079 exopolysaccharide, LA-EPS-20079, molecularly regulates both apoptotic and NF- $\kappa$ B inflammatory pathways in human colon cancer. *Microbial Cell Factories* **17**(1), 29 (2018).
27. Sasikumar, K., Kozhummil Vaikkath, D., Devendra, L. & Nampoothiri, K. M. An exopolysaccharide (EPS) from a *Lactobacillus plantarum* BR2 with potential benefits for making functional foods. *Bioresour. Technol.* **241**, 1152–1156 (2017).
28. Ayyash, M., Al-Nuaimi, A. K., Al-Mahadin, S. & Liu, S. Q. In vitro investigation of anticancer and ACE-inhibiting activity,  $\alpha$ -amylase and  $\alpha$ -glucosidase inhibition, and antioxidant activity of camel milk fermented with camel milk probiotic: A comparative study with fermented bovine milk. *Food Chem.* **239**, 588–597 (2018).
29. Jeong, D. *et al.* Characterization and antibacterial activity of a novel exopolysaccharide produced by *Lactobacillus kefirifaciens* DN1 isolated from kefir. *Food Control* **78**, 436–442 (2017).
30. Yang, X., Ren, Y., Zhang, L., Wang, Z. & Li, L. Structural characteristics and antioxidant properties of exopolysaccharides isolated from soybean protein gel induced by lactic acid bacteria. *LWT* **150**, 111811 (2021).
31. Li, M. *et al.* Structure characterization, antioxidant capacity, rheological characteristics and expression of biosynthetic genes of exopolysaccharides produced by *Lactococcus lactis* subsp. *lactis* IMAU11823. *Food Chem.* **384**, 132566 (2022).
32. Wu, Z. *et al.* Inflammation-related pro-apoptotic activity of exopolysaccharides isolated from *Lactococcus lactis* subsp. *lactis*. *Benef. Microbes* **7**(5), 761–768 (2016).
33. Nehal, F. *et al.* Characterization, high production and antimicrobial activity of exopolysaccharides from *Lactococcus lactis* F-mou. *Microb. Pathog.* **132**, 10–19 (2019).
34. Zhang, M., Che, Y. & Wu, C. A novel exopolysaccharide produced by *Zygosaccharomyces rouxii* with cryoprotective and freeze-drying protective activities. *Food Chem.* **392**, 133304 (2022).
35. Rajoka, M. S. R. *et al.* Techno-functional properties and immunomodulatory potential of exopolysaccharide from *Lactiplantibacillus plantarum* MM89 isolated from human breast milk. *Food Chem.* **377**, 131954 (2022).
36. Liu, Z. *et al.* Characterization and bioactivities of the exopolysaccharide from a probiotic strain of *Lactobacillus plantarum* WLPL04. *J. Dairy Sci.* **100**(9), 6895–6905 (2017).
37. Ma, W. *et al.* Characterization, antioxidant activity, and anti-carcinoma activity of exopolysaccharide extract from *Rhodotorula mucilaginosa* CICC 33013. *Carbohydr. Polym.* **181**, 768–777 (2018).
38. Xiao, L. *et al.* Biosynthesis of exopolysaccharide and structural characterization by *Lactocaseibacillus paracasei* ZY-1 isolated from Tibetan kefir. *Food Chem. Mol. Sci.* **3**, 100054 (2021).
39. Lundborg, M. & Widmalm, G. R. Structural analysis of glycans by NMR chemical shift prediction. *Anal. Chem.* **83**(5), 1514–1517 (2011).
40. Lo, T.C.-T., Chang, C. A., Chiu, K.-H., Tsay, P.-K. & Jen, J.-F. Correlation evaluation of antioxidant properties on the monosaccharide components and glycosyl linkages of polysaccharide with different measuring methods. *Carbohydr. Polym.* **86**(1), 320–327 (2011).
41. Nguyen, D. T. & Nguyen, T. H. Detection on antioxidant and cytotoxicity activities of exopolysaccharides isolated in plant-originated *Lactococcus lactis*. *Biomed. Pharmacol. J.* **7**(1), 33–38 (2015).
42. Pan, D. & Mei, X. Antioxidant activity of an exopolysaccharide purified from *Lactococcus lactis* subsp. *lactis* 12. *Carbohydr. Polym.* **80**(3), 908–914 (2010).
43. Sharma, P. *et al.* Emerging trends in the novel drug delivery approaches for the treatment of lung cancer. *Chem. Biol. Interact.* **309**, 108720 (2019).
44. Rajoka, M. S. R., Wu, Y., Mehwish, H. M., Bansal, M. & Zhao, L. *Lactobacillus* exopolysaccharides: New perspectives on engineering strategies, physiochemical functions, and immunomodulatory effects on host health. *Trends Food Sci. Technol.* **103**, 36–48 (2020).
45. Salachna, P., Mizielińska, M. & Soból, M. Exopolysaccharide gellan gum and derived oligo-gellan enhance growth and antimicrobial activity in *Eucomis* plants. *Polymers* **10**(3), 242 (2018).
46. Abdalla, A. K. *et al.* Exopolysaccharides as antimicrobial agents: Mechanism and spectrum of activity. *Front. Microbiol.* **12**, 664395 (2021).
47. Abid, Y. *et al.* Rheological and emulsifying properties of an exopolysaccharide produced by potential probiotic *Leuconostoc citreum*-BMS strain. *Carbohydr. Polym.* **256**, 117523 (2021).
48. Li, J. *et al.* Characterization of an exopolysaccharide with distinct rheological properties from *Paenibacillus edaphicus* NUST16. *Int. J. Biol. Macromol.* **105**, 1–8 (2017).
49. Medina-Cabrera, E. V., Gansbiller, M., Rühmann, B., Schmid, J. & Sieber, V. Rheological characterization of *Porphyridium sordidum* and *Porphyridium purpureum* exopolysaccharides. *Carbohydr. Polym.* **253**, 117237 (2021).

## Acknowledgements

Authors are thankful to United Arab Emirates University for funding this project via grant numbers 31F135 and 12R105. We thank NYUAD CTP for the access to the NMR facility.

## Author contributions

G.B., A.H.A., C.T.-R., & A.S.: Writing—Original Draft; G.E. & F.H.: Investigation; R.Y.G.: & S.-Q.L.: Writing—Review & Editing; B.A.-J.: Writing—Original Draft, Formal analysis, Writing—Review & Editing; M.A.: Conceptualization, Funding acquisition; Project administration, Investigation, Writing—Review & Editing.

## Competing interests

The authors declare no competing interests.

## Additional information

**Supplementary Information** The online version contains supplementary material available at <https://doi.org/10.1038/s41598-023-44728-w>.

**Correspondence** and requests for materials should be addressed to B.A.-J. or M.A.

**Reprints and permissions information** is available at [www.nature.com/reprints](http://www.nature.com/reprints).

**Publisher's note** Springer Nature remains neutral with regard to jurisdictional claims in published maps and institutional affiliations.



**Open Access** This article is licensed under a Creative Commons Attribution 4.0 International License, which permits use, sharing, adaptation, distribution and reproduction in any medium or format, as long as you give appropriate credit to the original author(s) and the source, provide a link to the Creative Commons licence, and indicate if changes were made. The images or other third party material in this article are included in the article's Creative Commons licence, unless indicated otherwise in a credit line to the material. If material is not included in the article's Creative Commons licence and your intended use is not permitted by statutory regulation or exceeds the permitted use, you will need to obtain permission directly from the copyright holder. To view a copy of this licence, visit <http://creativecommons.org/licenses/by/4.0/>.

© The Author(s) 2023